

This is a repository copy of *Differential transcription factor expression by human epithelial cells of buccal and urothelial derivation*.

White Rose Research Online URL for this paper:

<https://eprints.whiterose.ac.uk/131586/>

Version: Accepted Version

Article:

Southgate, Jennifer orcid.org/0000-0002-0135-480X, Hustler, Arianna, Eardley, Ian et al. (5 more authors) (2018) Differential transcription factor expression by human epithelial cells of buccal and urothelial derivation. *Experimental cell research*. pp. 284-294. ISSN 0014-4827

<https://doi.org/10.1016/j.yexcr.2018.05.031>

Reuse

This article is distributed under the terms of the Creative Commons Attribution-NonCommercial-NoDerivs (CC BY-NC-ND) licence. This licence only allows you to download this work and share it with others as long as you credit the authors, but you can't change the article in any way or use it commercially. More information and the full terms of the licence here: <https://creativecommons.org/licenses/>

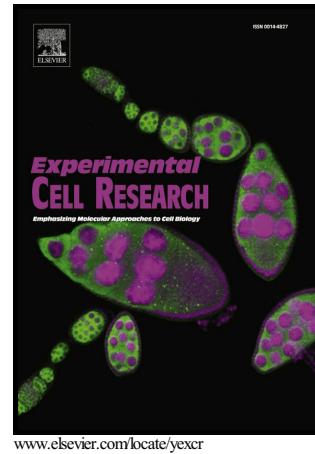
Takedown

If you consider content in White Rose Research Online to be in breach of UK law, please notify us by emailing eprints@whiterose.ac.uk including the URL of the record and the reason for the withdrawal request.

Author's Accepted Manuscript

Differential transcription factor expression by human epithelial cells of buccal and urothelial derivation

Arianna Hustler, Ian Eardley, Jennifer Hinley, Joanna Pearson, Felix Wezel, Francois Radvanyi, Simon C Baker, Jennifer Southgate



PII: S0014-4827(18)30302-1
DOI: <https://doi.org/10.1016/j.yexcr.2018.05.031>
Reference: YEXCR11055

To appear in: *Experimental Cell Research*

Received date: 8 December 2017
Revised date: 24 May 2018
Accepted date: 25 May 2018

Cite this article as: Arianna Hustler, Ian Eardley, Jennifer Hinley, Joanna Pearson, Felix Wezel, Francois Radvanyi, Simon C Baker and Jennifer Southgate, Differential transcription factor expression by human epithelial cells of buccal and urothelial derivation, *Experimental Cell Research*, <https://doi.org/10.1016/j.yexcr.2018.05.031>

This is a PDF file of an unedited manuscript that has been accepted for publication. As a service to our customers we are providing this early version of the manuscript. The manuscript will undergo copyediting, typesetting, and review of the resulting galley proof before it is published in its final citable form. Please note that during the production process errors may be discovered which could affect the content, and all legal disclaimers that apply to the journal pertain.

Differential transcription factor expression by human epithelial cells of buccal and urothelial derivation.

Arianna Hustler¹, Ian Eardley², Jennifer Hinley¹, Joanna Pearson¹, Felix Wezel¹¹, Francois Radvanyi³, Simon C Baker¹ & Jennifer Southgate^{1*}.

¹Jack Birch Unit for Molecular Carcinogenesis, Department of Biology, University of York, York YO10 5DD, United Kingdom.

²Pyrah Department of Urology, St. James's University Hospital, Leeds LS9 7TF, United Kingdom.

³Oncologie Moléculaire, Institut Curie, Centre de Recherche, 75248 cedex 05, Paris, France

***Contact Information:** Corresponding author: j.southgate@york.ac.uk

¹ Current address: Department of Urology, Ulm University, Ulm, Germany

Abstract:

Identification of transcription factors expressed by differentiated cells is informative not only of tissue-specific pathways, but to help identify master regulators for cellular reprogramming. If applied, such an approach could generate healthy autologous tissue-specific cells for clinical use where cells from the homologous tissue are unavailable due to disease. Normal human epithelial cells of buccal and urothelial derivation maintained in identical culture conditions that lacked significant instructive or permissive signalling cues were found to display inherent similarities and differences of phenotype. Investigation of transcription factors implicated in driving urothelial-type differentiation revealed buccal epithelial cells to have minimal or absent expression of *PPARG*, *GATA3* and *FOXA1* genes. Retroviral overexpression of *GATA3* or *PPARG1* coding sequences in buccal epithelial cells resulted in nuclear immunolocalisation of the respective proteins, with both transductions also inducing expression of the urothelial differentiation-associated claudin 3 tight junction protein. *PPAR γ 1* overexpression alone entrained expression of nuclear *FOXA1* and *GATA3* proteins, providing objective evidence of its upstream positioning in a transcription factor network and identifying it as a candidate factor for urothelial-type transdifferentiation or reprogramming.

Key Words:

urothelium; buccal epithelium; transdifferentiation; nuclear receptor; transcription factor

Introduction:

The urinary tract from the renal pelvis, through ureters, bladder and proximal urethra is lined intra-luminally by urothelium: a transitional epithelium. Urothelium derives from two embryological sources: bladder urothelium is endodermally-derived from the urinogenital sinus, whereas ureteric urothelium is of mesodermal (Wolffian duct) origin (Tanaka et al., 2010). Both urothelia share common features of form and function, with stratification into basal, intermediate and the highly-specialised lumen-facing superficial cells that constitute the main urinary barrier. Superficial cells are characterised by apical expression of tissue-restricted transmembrane uroplakins that contribute to transcellular barrier function (Deng et al., 2002; Sun et al., 1996), whilst paracellular barrier function is provided by well-developed intercellular tight junctions (Van Itallie and Anderson, 2014; Varley et al., 2006). In human urothelium, expression of claudin 3 is implicated functionally in the terminal tight junction (Smith et al., 2015). Not only does urothelium form one of the tightest barriers in the body, but despite being mitotically-quiescent in the normal state, it is one of the most rapidly repairing of all mammalian tissues (reviewed by Khandelwal et al., 2009). The mechanism(s) involved in regulating the balance between urothelial differentiation and regeneration represent a paradox with major implications for urological practice.

There is a clinical need to reconstruct the lower urinary tract in patients with end-stage bladder diseases, including cancer (reviewed by Garriboli et al., 2014). In current surgical practices where the bladder is reconstructed with bowel (enterocystoplasty or cystectomy with urinary diversion using bowel), the large majority of complications arise from the incompatibility of bowel epithelium to long-term urine exposure (Froehner et al., 2009; Hautmann et al., 2006; Kälble et al., 2011). Alternative tissue engineering strategies for bladder replacement and lower urinary tract reconstruction are at different stages of development and translation (Adamowicz et al., 2017; Lam Van Ba et al., 2015; Turner et al., 2011). In all approaches, the need for a functional urinary barrier is paramount to avoid

serious clinical complications. As a patient's own urothelium may be compromised by disease or the disease environment (Subramaniam et al., 2011), the ability to generate urothelium from induced pluripotent or other autologous cells is an essential, albeit future goal.

We have previously described a cell culture system for propagating normal human urothelial (NHU) cells in low calcium, serum-free medium (Southgate et al., 1994). In these conditions, urothelial cells lose expression of archetypical transitional epithelial markers (including cytokeratin (CK) 13, differentiation-restricted CK20 and most uroplakin genes) and adopt a more primitive or "basal-like" EGFR-autocrine-regulated CK14-positive squamous epithelial cell phenotype (Varley et al., 2005). Such cells retain capacity for urothelial-type differentiation, inducible either by ligand-activation of PPAR γ (Varley et al., 2004b, 2004a, 2009), or by growth in serum (Cross et al., 2005). Applied to bladder or ureteric human urothelial cells, both methods promote a common network of transcription factors (TFs) (Böck et al., 2014) that further induce the differentiation-associated expression of urothelial cytokeratins, tight junction claudins and uroplakins (Varley et al., 2004b, 2004a, 2006). Specified TFs of the network, including interferon regulatory factor 1 (IRF1), forkhead box protein A1 (FOXA1), E74-like factor 3 (ELF3) and GATA Binding Protein 3 (GATA3), have been verified to have a functional role in transactivating the downstream differentiation-associated genes (Böck et al., 2014; Fishwick et al., 2017; Varley et al., 2009). Further evidence of a causal influence on urothelial programming is the finding that many of these same TF genes are implicated in urothelial cancer (Choi et al., 2014; Eriksson et al., 2015; The Cancer Genome Atlas Research Network, 2014).

It is axiomatic that the precise nature of the transcription factor networks will specify the differentiated phenotype. Therefore, we sought to identify key urothelium-determining TFs by comparing to oral epithelial cells from buccal mucosa. We proposed to use the identified

constitutive differences in TF expression to perform a preliminary investigation into the influence of ectopic TF expression on the interconversion of oral epithelial into urothelial cells. As in other systems, where a transdifferentiation approach has informed the master cell type regulators (eg myogenic differentiation (MyoD) (Davis et al., 1987)), such an approach is predicted to identify the key factors required for urothelial conversion from pluripotent stem cell sources.

Materials and Methods:

Tissue Samples

The collection and use of human tissues for research was covered by NHS Research Ethics Committee approvals, with patient informed consent as required. Buccal mucosa tissue samples were obtained as trimmings from male patients (age 3-65) undergoing urethral repair surgery. Urothelial samples (from renal pelvis or ureter) were obtained from anonymous male and female donors (age 1-79 years) undergoing a variety of urological procedures, including uninvolved urothelial tissue distal to renal cell carcinoma. Histological analysis on representative fragments was performed to check that all tissue samples were of normal morphology.

Cell Culture

Normal human buccal epithelial (NHB) cells and normal human urothelial (NHU) cells were isolated as described (Oda and Watson, 1990; Southgate et al., 1994) respectively. In brief, to isolate NHB cells, first the epithelium was separated from the underlying connective tissue by incubation in 0.5 % (w/v) Dispase II (Roche) at 37 °C for 3-4 hours. The epithelium was dissected into small pieces with scissors and the cells dissociated by incubation in a trypsin-EDTA solution at 37 °C for 5 minutes. For NHU cell isolation, tissue samples were incubated in an EDTA containing solution for 4 hours at 37 °C. The epithelium, following separation

from the underlying connective tissue using forceps, was incubated in 100 U/ml collagenase (type IV) for 20 min at 37 °C. Following the isolations, primary NHB and NHU cells were cultured identically on Primaria™ plasticware (Corning) in keratinocyte serum-free medium (KSFM) containing bovine pituitary extract (BPE) and epidermal growth factor (EGF) (Invitrogen) plus 30 ng/ml cholera toxin. NHB and NHU cell cultures were passaged at just-confluence and maintained as serially-passaged finite cell lines, as previously described for NHU cells (Southgate et al., 1994). Each experiment was performed on one to four independent donor cell lines, with a total of 16 independent NHB donor cell lines and 10 independent NHU donor cell lines used to perform the experiments described herein. The number (n) of independent cell lines used for each experiment is provided in the respective figure legends.

Urothelial Differentiation Protocols

Two protocols optimised previously for the differentiation of NHU cells were applied for the differentiation experiments reported here; NHU cells cultured identically to the NHB cells were included as comparative controls.

First, to induce differentiation by PPAR γ activation, 70 % confluent epithelial (NHU control or NHB) cell cultures were exposed to 1 μ M PD153035 (EGFR-TK inhibitor) (Merck Millipore) and 1 μ M troglitazone (TZ; PPAR γ agonist) (Tocris) for 24 hours, before replacement with 1 μ M PD153035 alone (protocol termed TZ/PD) (Varley et al., 2004a).

Second, to produce stratified epithelial cell sheets, epithelial (NHU control or NHB) cell cultures were grown to 80% confluence and the medium was changed to contain 5% (v/v) adult bovine serum (ABS; SeraLab) for five days. For TEER studies, the cultures were then passaged and seeded onto 12 mm, 0.4 μ m pore-size Snapwell culture inserts (Corning® Costar®). The insert cultures were established in medium containing 5 % ABS for 24 hours and the medium was changed to contain 5 % ABS plus 2 mM [Ca²⁺] (Cross et al., 2005).

Barrier Assessment and Cell Sheet Harvest

Trans-Epithelial Electrical Resistance (TEER) measurements were taken using chopstick STX2 electrodes and an Epithelial Voltometer (World Precision Instruments). The average TEER of Snapwell culture inserts containing medium only was subtracted from each recorded value. To harvest epithelial cell sheets from the Snapwell culture inserts, cell sheets were incubated with 2% (w/v) Dispase II (Roche) for 30 minutes at 37 °C. Released cell sheets were floated into CellSafe+ biopsy capsules (CellPath) and placed into embedding cassettes. The cell sheets were fixed in 4 % formaldehyde for 24 hours, before processing into paraffin wax.

Antibodies

The following primary antibodies were used at the stated titrations for immunoblotting (IB), immunofluorescence (IF) and immunohistochemistry (IHC): β -actin (ACTB; Sigma-Aldrich, AC-15) (IB – 1:250,000); claudin 3 (Life Technologies, Z23.JM) (IB – 1:4000); claudin 4 (Life Technologies, 3E2C1) (IB – 1:1000); claudin 5 (Life Technologies, 4C3C2) (IB – 1:1000); claudin 7 (Life Technologies, ZMD.241) (IB – 1:1000); cytokeratin 5 (CK5) (Abcam, SP27) (IHC – 1:100); cytokeratin 5 (CK5) (The Binding Site, PH607) (IF – 1:100); cytokeratin 7 (CK7) (Novocastra, OV-TL12/30) (IHC – 1:400, IF – 1:40); cytokeratin 13 (CK13) (Abnova, 1C7) (IHC – 1:500, IF – 1:500); cytokeratin 14 (CK14) (Serotec, LL002) (IHC – 1:1200); cytokeratin 14 (CK14) (ICRF, LL001) (IF – 1:5); cytokeratin 20 (CK20) (Novocastra, Kr20.8) (IHC – 1:200); Cytokeratin 20 (CK20) (Cymbus Bioscience, IT-Ks20.3) (IF – 1:100); ELF3 (Abcam, EPESER1) (IF – 1:1000, IB – 1:20,000); FOXA1 (Santa Cruz Biotechnology, Q-6) (IF – 1:200, IB – 1:500); FOXA1/2 (Santa Cruz Biotechnology, C-20) (IF – 1:200); GATA3 (Cell Signaling, D13C9) (IF – 1:800, IB – 1:1000); PPARG (Cell Signaling, D69) (IF – 1:100, IB – 1:500).

Immunohistochemistry (IHC)

5 µm sections were dewaxed through xylene into ethanol. Antigen retrieval was performed by boiling the slides in 10 mM citric acid buffer (pH 6.0) for 10 minutes. For some antibodies (CK13 and CK14), cell sheets were incubated in 0.1 % trypsin at 37 °C prior to the citric acid incubation. Sections were blocked using an avidin/biotin blocking kit (Vector Laboratories) and 5 % rabbit or goat serum (as determined by the secondary antibody), incubated with primary antibody at 4 °C overnight, then washed. A biotinylated secondary antibody was applied to the cell sheets, followed by a streptavidin-biotinylated/horseradish peroxidase complex (Vector Laboratories), before visualisation with diaminobenzidine (Sigma Aldrich). The cell sheets were counterstained lightly with haematoxylin, dehydrated and mounted in DPX (CellPath). Appropriate methodology, specificity and negative controls were included for each antibody.

Reverse Transcribed-Polymerase Chain Reaction (RT-PCR) and quantitative RT-PCR (RT-qPCR).

Cell cultures were solubilised using TRIzol™ Reagent and RNA extraction was performed using a phenol-chloroform and isopropanol precipitation method according to the manufacturer's instructions (Invitrogen). Any contaminating genomic DNA was removed by DNase digestion (DNA-free™, Ambion) and checked using RT-negative controls. cDNA was synthesized from 1 µg of total RNA using the first-strand synthesis system primed with random hexamers (Invitrogen). RT-PCR and RT-qPCR were performed as described previously (Böck et al., 2014). A list of PCR primers is provided in Table 1. RT-qPCR was performed using three technical replicates for each gene. RT-PCR was performed using 30 cycles except for GAPDH (25 cycles).

Immunoblotting

Whole protein lysates were generated from cell cultures using a reducing 2x SDS lysis buffer containing 1% protease inhibitor (Sigma-Aldrich). Lysates were incubated on ice for 30 minutes and centrifuged at 20,000 g for 30 minutes at 4 °C. 25 µg was loaded into either 4-12 % bis-Tris gels or 3-8 % Tris-acetate gels (Novex®) and electrophoresis was performed at 200 V for 1 hour. Proteins were transferred to an Immobilon-FL 0.45 µm PVDF membrane by electroblotting. Membranes were blocked using Odyssey Blocking Buffer (Li-Cor) and incubated with the primary antibody overnight at 4 °C. The fluorescent secondary antibody was applied to the membrane for 1 hour at ambient temperature, and membranes were imaged for semi-quantification using an Odyssey® infrared imaging system (Li-Cor).

Immunofluorescence Microscopy

Cells were cultured on 12-well glass slides (C A Hendley Essex Ltd), fixed in 4 % formaldehyde for 10 minutes and permeabilised with 0.1 % Triton™ X-100 (Sigma Aldrich), before incubation with primary antibody in a 0.1% BSA solution overnight at 4 °C. A fluorescent-conjugated secondary antibody was applied to the cells for 1 hour at ambient temperature, before further washing and counterstaining of nuclei with 0.1 µg/ml Hoechst 33258 (Sigma Aldrich).

Overexpression of GATA3 and PPARG1 in NHB cells by Retroviral Transduction

Sequences for *GATA3* (CCDS31143) and *PPARG1* (CCDS2610) were cloned into the retroviral vector, pLXSN (Clontech) and confirmed by sequencing. pLXSN-*GATA3* and pLXSN-*PPARG1* plasmids were transfected into retroviral packaging cells (PT67 cells) (Clontech), and selected with G418. Successfully transfected PT67 cells were grown to confluence and the generated retrovirus was collected in the medium. NHB cells were

transduced with the retrovirus and successfully transduced epithelial cells were selected using antibiotics. Control NHB cells were transduced with the pLXSN vector only (Empty).

Statistical Analysis

Statistical analysis was performed where appropriate using either a two-tailed, paired t-test or a one-way ANOVA with post-test. Error bars represent standard deviation.

Accepted manuscript

Results

Comparison of Human Urothelial and Buccal Epithelial Phenotypes In Situ and In Vitro.

In situ, the epithelium of buccal mucosa is a non-cornified stratified squamous epithelium that can average 30 cell layers thick. By contrast, the urothelium, a transitional epithelium, averages 4-5 cell layers. Immunohistochemical examination of CK5, CK7, CK13, CK14 and CK20 revealed expression of CK5 in all layers of buccal epithelium and an absence of CK7 and CK20 expression. CK13 expression was suprabasal, whilst CK14 was particularly intense but not exclusive to the basal layers of buccal epithelium (Fig. 1A). In urothelium, CK5 and CK13 were associated with the basal layers, CK7 was present in all layers, CK14 was absent and CK20 was confined to the superficial cell layer (Fig. 1B).

When isolated and maintained in identical low calcium [0.09 mM] serum-free culture conditions (Fig. 1C), both NHU and NHB cells formed proliferative, contact-inhibited monolayer cultures that upon reaching confluence could be serially sub-cultured up to 10 times (data not shown). The *in vitro* expression of cytokeratin proteins by both cell types was similar by immunocytochemistry, with CK5, CK7, CK13 and CK14 detected, including gain of CK7 by NHB cells and gain of CK14 by NHU cells; CK20 was not expressed (Fig. 1D).

Generation of Cell Sheets and Measurement of Barrier Function

Using a protocol optimised for differentiated barrier induction by NHU cells *in vitro* (Cross et al., 2005), NHB cultures formed multi-layered cell sheets that were similar morphologically to those achieved by NHU cells cultured in identical conditions (Fig. 2A). Using TEER to assess barrier function, NHB cell sheets were unable to form a tight barrier (defined here as $\geq 1 \text{ k}\Omega \cdot \text{cm}^2$), compared to typical barriers formed by NHU cells of 3 to 5 $\text{k}\Omega \cdot \text{cm}^2$ (Fig. 2B). Immunohistochemical analysis of cytokeratin expression in NHB cell sheets demonstrated

consistent expression of CK5 and CK14 throughout all layers, with CK13 limited to the upper portion of the cell sheets, and diffuse, weak CK7 expression (Fig. 2C). By contrast, NHU cell sheets were CK7-positive throughout all cell layers and demonstrated reciprocal patterns of CK5 and CK13, but were negative for CK14.

Expression of Uroplakin (UPK) Genes by NHB Cells In Vitro

Uroplakin transcript expression was evaluated initially by RT-PCR in control NHB cell cultures and following combined TZ/PD treatment (Fig. S1) (Varley et al., 2004a). NHB cells showed robust expression of *UPK1B* and *UPK3B*, with equivocal expression of *UPK1A* and *UPK2* appearing at later (confluence-associated) time-points in both baseline and induced conditions (Fig. S1). These results were confirmed by RT-qPCR in three independent NHB donor cell lines, where NHB cells were shown to express transcripts for *UPK1A*, *UPK1B*, *UPK2* and *UPK3B* (Fig. 3A). The expression of *UPK2* and *UPK3B* transcripts by NHB cells was significantly upregulated at 72 hours following combination TZ/PD therapy (Fig. 3A). Expression of *UPK3A* was absent in NHB cells.

Expression of Urothelial Differentiation-Associated Transcription Factors by NHB Cells In Vitro.

Based on the clear phenotypic differences observed between the two cell types *in vitro*, RT-PCR was used to evaluate expression of seven transcription factor genes (*ELF3*, *FOXA1*, *GATA3*, *GRHL3*, *KLF5*, *IRF1* and *PPARG*) implicated in urothelial development and/or differentiation (Bell et al., 2011; Böck et al., 2014; Varley et al., 2004b, 2004a, 2006, 2009; Yu et al., 2009) (Fig. 3B&C). NHB cells showed absent or barely-detectable expression of *FOXA1*, *GATA3* and *PPARG* transcripts even following attempts using TZ/PD to initiate differentiation in case of a positive feedback loop. Expression of *GRHL3*, *IRF1* and

KLF5 appeared constitutive in nature, while *ELF3* expression was upregulated in response to TZ/PD.

RTqPCR analysis of three independent NHB donor cell lines confirmed the results obtained by RT-PCR, demonstrating weak expression of *FOXA1*, *GATA3* and *PPARG*, with significant upregulation only of *ELF3* transcript following TZ/PD treatment (Fig. 4A). Similar results were obtained by evaluating protein expression by western blotting (Fig. 4B). By immunofluorescence microscopy, *ELF3*, *FOXA1/2*, *GATA3* and *PPAR γ 1* were weak/absent in NHB cells treated with combined TZ/PD, contrasting to the typically strong nuclear protein expression seen when NHU cells were subjected to identical conditions *in vitro* (Fig. 4C).

NHB overexpression studies.

To further investigate transcription factor regulation and hierarchies, *GATA3* and *PPARG1* were selected to stably overexpress in NHB cells due to their low/absent expression in NHB cells and known expression and importance in urothelial differentiation. *PPARG1* was selected over *PPARG2* due to previous evidence suggesting that *PPAR γ 1* is the primary *PPARG* isoform required for urothelial cell-type differentiation (Strand et al., 2013).

GATA3

Successful overexpression of *GATA3* was achieved in NHB cells and resulting in nuclear immunolocalisation (Fig. 5A&B). Overexpression of *GATA3* did not cause any noticeable effect on *FOXA1* or *PPAR γ 1* protein expression in NHB cells, as shown by both western blotting and immunofluorescence microscopy (Fig. 5A&B). This remained true even following attempts to activate *PPAR γ* by combined TZ/PD treatment. Expression of tight junction-associated proteins was examined when transduced NHB cells were induced to form cell sheets using 5% bovine serum and 2 mM [Ca^{2+}]. A clear upregulation of claudin 3 protein expression was observed following *GATA3* overexpression in NHB cells (Fig. 5C).

Expression of other urothelium-associated tight junction proteins, claudins 4, 5 and 7 were

expressed consistently in both control (Empty vector) and *GATA3* overexpressing NHB cells. *GATA3* overexpression, and subsequent Claudin 3 upregulation, failed to result in the gain of barrier function by NHB cells sheets, as measured by TEER ($81.74 \pm 2.35 \Omega \cdot \text{cm}^2$, Day 4, n=3; Control: $110.36 \pm 3.54 \Omega \cdot \text{cm}^2$, Day 4, n=3).

PPARG1

Overexpression of *PPARG1* in NHB cells caused a noticeable increase in FOXA1 protein expression by western blotting (Fig. 6A), although this was not significant when quantified across transductions in four independent NHB lines (Fig. 6B). *GATA3* protein expression was poorly detectable by western blotting in *PPARG1* overexpressing NHB cells, even following attempts to activate PPAR γ using combination TZ/PD treatment. However, by immunofluorescence microscopy *PPARG1* overexpression resulted in clear *de novo* nuclear localisation of PPAR γ (n=3/3), FOXA1 (n=3/3) and *GATA3* (n=2/3) (Fig. 6C).

Evaluation of tight junction-associated proteins following stratification of transduced NHB cells, revealed a significant upregulation of Claudin 3 protein expression (Fig. 7A&B). The expression of Claudins 4, 5 and 7 remained consistently expressed in both control (empty vector) and *PPARG1*-overexpressing cells (Fig. 7A). In addition, *PPARG1* overexpression had no effect on CK14 expression, which was detectable in both control (empty vector) and *PPARG1* overexpressing NHB cells (Fig. 7C). Finally, *PPARG1* overexpression did not result in the gain of barrier function in NHB cell sheets, as measured by TEER ($54.24 \pm 2.99 \Omega \cdot \text{cm}^2$, Day 4, n=3; Control: $15.82 \Omega \cdot \text{cm}^2$, Day 4, n=2).

Discussion:

In this study we have used a different epithelial cell type in experiments aimed at informing future strategies for programming autologous cells to generate human urothelium. Our study has shown that PPAR γ 1 and GATA3 are nuclear factors differentially expressed by human urothelial, not buccal, epithelial cells and that when expressed as individual transgenes, these factors effect specific changes on buccal epithelial cell phenotype.

Various groups have attempted to generate human urothelial cells from different types of stem cells in order to identify a surrogate cell source for autologous bladder tissue engineering (reviewed by Chan et al., 2017). The initiating human cell sources investigated have included bone marrow-derived mesenchymal stem cells (Tian et al., 2010); adipose-derived stem cells (Shi et al., 2012); amniotic fluid-derived stem cells (Kang et al., 2014a); umbilical cord stem cells (Wu et al., 2013); pluripotent embryonic stem cells (Osborn et al., 2014); induced pluripotent stem cells (iPSCs) (Kang et al., 2014b; Moad et al., 2013); and voided urine cells (Zhang et al., 2008). The inducing method has frequently assumed production of unidentified instructive paracrine factors by urothelial or bladder cancer cell lines employed in co-culture (Chung and Koh, 2013; Liu et al., 2009; Ning et al., 2011; Tian et al., 2010), or via medium-conditioning (Kang et al., 2014a; Moad et al., 2013; Shi et al., 2012; Wu et al., 2013; Zhao et al., 2014). Collectively, the results suggest that from any naïve heterotypic starting population, an unknown proportion of cells will express urothelial differentiation-associated genes under permissive conditions.

More systematic attempts have used a two-staged approach in which pluripotent stem cells of embryonic (Osborn et al., 2014) or iPSC (Kang et al., 2014b) derivation are first differentiated into definitive endoderm cells. This is followed by attempts to direct urothelial differentiation using agonists that activate PPAR γ (Osborn et al., 2014) or the retinoic acid

receptor (RAR) (Kang et al., 2014b), as candidate nuclear receptors whose activation is implicated in urothelial differentiation.

Irrespective of the approach, all above studies have reported qualitatively similar outcomes in detecting upregulated epithelial- and urothelial-associated gene expression within the emergent population. Fold increases in the expression of uroplakin (UPK) genes has been presented as *prima facie* evidence of urothelial conversion, even though it is well established that uroplakin transcripts are expressed by other (non-urothelial) epithelial cell types (Adachi et al., 2000; Kanamori-Katayama et al., 2011; Olsburgh et al., 2003; Rudat et al., 2014). UPK1B and UPK3B are the least differentiation stage-restricted of the uroplakins in urothelium and here, buccal epithelial cells *in vitro* were shown clearly to express both *UPK1B* and *UPK3B* transcripts. Transcripts for *UPK1A* and *UPK2*, which are more differentiation stage-restricted in urothelium, were also, albeit variably, expressed by buccal epithelial cells, further establishing that expression of uroplakin gene transcripts alone cannot be used to definitively mark urothelium-specific conversion. Only *UPK3A* expression was absent from native buccal epithelial cells *in vitro*, potentially indicating that *UPK3A* expression could represent a more objective marker of successful (re)programming to differentiated urothelium. This study further indicated the absence of CK14 and expression of CLDN3 as part of the urothelial signature phenotype.

We have previously shown that maintenance of NHU cells *in vitro* in a low calcium, serum-free medium results in the loss of urothelial phenotype and reversion to a more primitive squamous state, accompanied by changes in chromatin organisation (Fishwick et al., 2017). Under identical serum-free culture conditions, buccal epithelial cells similarly adopt a proliferative, non-stratified CK14+ squamous phenotype. The provision of serum, in conjunction with physiological calcium to promote development of intercellular junctions and

polarity, led to re-establishment of the original differentiation programmes of urothelial and buccal cells, respectively, indicating that despite the apparent plasticity, cultured cells perhaps retained an epigenetic “memory”. The addition of serum provides a permissive environment for differentiation, revealing underpinning differences in epithelial lineage programming, with urothelial cells switching to a CK13⁺ transitional programme, whereas buccal epithelial cells maintain the CK14⁺ stratified squamous programme.

A comparison of TF expression between buccal versus urothelial cells revealed differential expression of FOXA1, GATA3 and PPAR γ . In preadipocytes, ligand activation of PPAR γ protein provokes transactivation of *PPARG* as a differentiation-inducing positive feedback event (Mueller et al., 2002). This led us to investigate whether ligand-induced activation of PPAR γ in wild type buccal epithelial cells could alone entrain a urothelial-like differentiation response as part of a positive feedback response. However, in the event, it failed to initiate expression of PPAR γ , FOXA1 or GATA3, further supporting the idea that inherent or programmed differences between cells (rather than perhaps the presence of inducing ligands) defines lineage/differentiation potential. Whereas forced overexpression of *GATA3* alone failed to have any clear impact on the expression of PPAR γ or FOXA1 in buccal epithelial cells, forced expression of *PPARG1* did promote both FOXA1 and GATA3 expression, indicating an upstream position in the regulatory network.

The primary function of the urothelium is to act as a barrier to urine and even following propagation *in vitro*, urothelium-derived cells retain the capacity to differentiate to form a functional barrier epithelium. We have shown here that when maintained under identical serum-containing culture conditions, *in vitro*-propagated buccal epithelial cells can form a stratified epithelial structure, whilst failing to form a functional barrier. The claudins are the main functional barrier-determining constituent of the tight junction, and claudin 3, which has

been identified previously as a critical tight junction protein required (but not sufficient) for urothelial barrier function (Smith et al., 2015), was weakly expressed in wild type buccal epithelial cells. Our approach has demonstrated that individual overexpression of GATA3 and PPAR γ 1 are both able to promote increased claudin 3 protein expression in buccal epithelial cells, providing circumstantial evidence implicating them in the urothelial differentiation and barrier formation programme.

To date, no study has completely defined the conditions or factors required to direct pluripotent cells into coherent urothelial cells capable of forming a functional urinary barrier. This suggests a need for better criteria to inform and monitor the process of successful urothelial cell programming. Here, we have brought some clarity to the order of complex endogenous TF relationships likely to be operating in urothelial cells, where there is both interplay between TFs at the level of cooperativity and competition for DNA binding, along with positive and negative feedback on TF transcription regulation (Fishwick et al., 2017). In conclusion, our results support PPAR γ 1 as a key upstream regulator that could constitute a component of a minimal transcription factor network required to promote urothelial-type differentiation. As buccal epithelial cells were shown to retain constitutive differences of phenotype in serum-free (non-permissive) culture conditions, we suggest that *PPARG1* overexpression experiments in (induced) pluripotent cells would be an informative next step for the programmed production of urothelial cells for therapy.

References:

Adachi, W., Okubo, K., and Kinoshita, S. (2000). Human uroplakin Ib in ocular surface epithelium. *Investig. Ophthalmol. Vis. Sci.* *41*, 2900–2905.

Adamowicz, J., Pokrywczyńska, M., Van Breda, S.V., Kloskowski, T., and Drewa, T. (2017). Concise Review: Tissue Engineering of Urinary Bladder; We Still Have a Long Way to Go? *Stem Cells Transl. Med.* *6*, 2033–2043.

Bell, S.M., Zhang, L., Mendell, A., Xu, Y., Haitchi, H.M., Lessard, J.L., and Whitsett, J.A. (2011). Kruppel-like factor 5 is required for formation and differentiation of the bladder urothelium. *Dev. Biol.* *358*, 79–90.

Böck, M., Hinley, J., Schmitt, C., Wahlicht, T., Kramer, S., and Southgate, J. (2014). Identification of ELF3 as an early transcriptional regulator of human urothelium. *Dev. Biol.* *386*, 321–330.

Chan, Y., Sandlin, S., Kurzrock, E., and Osborn, S. (2017). The Current Use of Stem Cells in Bladder Tissue Regeneration and Bioengineering. *Biomedicines* *5*, 4.

Choi, W., Porten, S., Kim, S., Willis, D., Plimack, E.R., Hoffman-Censits, J., Roth, B., Cheng, T., Tran, M., Lee, I.L., et al. (2014). Identification of Distinct Basal and Luminal Subtypes of Muscle-Invasive Bladder Cancer with Different Sensitivities to Frontline Chemotherapy. *Cancer Cell* *25*, 152–165.

Chung, S.S., and Koh, C.J. (2013). Bladder cancer cell in co-culture induces human stem cell differentiation to urothelial cells through paracrine FGF10 signaling. *Vitr. Cell. Dev. Biol. - Anim.* *49*, 746–751.

Cross, W.R., Eardley, I., Leese, H.J., and Southgate, J. (2005). A biomimetic tissue from cultured normal human urothelial cells: analysis of physiological function. *Am. J. Physiol. Renal Physiol.* *289*, F459–F468.

Davis, R.L., Weintraub, H., and Lassar, A.B. (1987). Expression of a single transfected

cDNA converts fibroblasts to myoblasts. *Cell* 51, 987–1000.

Deng, F.M., Liang, F.X., Tu, L., Resing, K.A., Hu, P., Supino, M., Hu, C.C.A., Zhou, G., Ding, M., Kreibich, G., et al. (2002). Uroplakin IIIb, a urothelial differentiation marker, dimerizes with uroplakin Ib as an early step of urothelial plaque assembly. *J. Cell Biol.* 159, 685–694.

Eriksson, P., Aine, M., Veerla, S., Liedberg, F., Sjödaahl, G., and Höglund, M. (2015).

Molecular subtypes of urothelial carcinoma are defined by specific gene regulatory systems. *BMC Med. Genomics* 8, 25.

Fishwick, C., Higgins, J., Percival-Alwyn, L., Hustler, A., Pearson, J., Bastkowski, S., Moxon, S., Swarbreck, D., Greenman, C.D., and Southgate, J. (2017). Heterarchy of transcription factors driving basal and luminal cell phenotypes in human urothelium. *Cell Death Differ.*

Froehner, M., Brausi, M.A., Herr, H.W., Muto, G., and Studer, U.E. (2009). Complications Following Radical Cystectomy for Bladder Cancer in the Elderly. *Eur. Urol.* 56, 443–454.

Garriboli, M., Radford, A., and Southgate, J. (2014). Regenerative medicine in urology. *Eur. J. Pediatr. Surg.* 24, 227–236.

Hautmann, R.E., Volkmer, B.G., Schumacher, M.C., Gschwend, J.E., and Studer, U.E. (2006). Long-term results of standard procedures in urology: The ileal neobladder. *World J. Urol.* 24, 305–314.

Van Itallie, C.M., and Anderson, J.M. (2014). Architecture of tight junctions and principles of molecular composition. *Semin. Cell Dev. Biol.* 36, 157–165.

Kälble, T., Hofmann, I., Riedmiller, H., and Vergho, D. (2011). Tumor growth in urinary diversion: A multicenter analysis. *Eur. Urol.* 60, 1081–1086.

Kanamori-Katayama, M., Kaiho, A., Ishizu, Y., Okamura-Oho, Y., Hino, O., Abe, M., Kishimoto, T., Sekihara, H., Nakamura, Y., Suzuki, H., et al. (2011). LRRN4 and UPK3B are markers of primary mesothelial cells. *PLoS One* 6.

- Kang, H.H., Kang, J.J., Kang, H.G., and Chung, S.S. (2014a). Urothelial differentiation of human amniotic fluid stem cells by urothelium specific conditioned medium. *Cell Biol. Int.* **38**, 531–537.
- Kang, M., Kim, H.H., and Han, Y.M. (2014b). Generation of bladder urothelium from human pluripotent stem cells under chemically defined serum- and feeder-free system. *Int. J. Mol. Sci.* **15**, 7139–7157.
- Khandelwal, P., Abraham, S.N., and Apodaca, G. (2009). Cell biology and physiology of the uroepithelium. *Am. J. Physiol. Renal Physiol.* **297**, F1477-501.
- Lam Van Ba, O., Aharony, S., Loutochin, O., and Corcos, J. (2015). Bladder tissue engineering: A literature review. *Adv. Drug Deliv. Rev.* **82**, 31–37.
- Liu, J., Huang, J., Lin, T., Zhang, C., and Yin, X. (2009). Cell-to-cell contact induces human adipose tissue-derived stromal cells to differentiate into urothelium-like cells in vitro. *Biochem. Biophys. Res. Commun.* **390**, 931–936.
- Moad, M., Pal, D., Hepburn, A.C., Williamson, S.C., Wilson, L., Lako, M., Armstrong, L., Hayward, S.W., Franco, O.E., Cates, J.M., et al. (2013). A novel model of urinary tract differentiation, tissue regeneration, and disease: Reprogramming human prostate and bladder cells into induced pluripotent stem cells. *Eur. Urol.* **64**, 753–761.
- Mueller, E., Drori, S., Aiyer, A., Yie, J., Sarraf, P., Chen, H., Hauser, S., Rosen, E.D., Ge, K., Roeder, R.G., et al. (2002). Genetic Analysis of Adipogenesis through Peroxisome Proliferator-activated Receptor Isoforms. *J. Biol. Chem.* **277**, 41925–41930.
- Ning, J., Li, C., Li, H., and Chang, J. (2011). Bone marrow mesenchymal stem cells differentiate into urothelial cells and the implications for reconstructing urinary bladder mucosa. *Cytotechnology* **63**, 531–539.
- Oda, D., and Watson, E. (1990). Human Oral Epithelial Cell Culture I. Improved Conditions for Reproducible Culture in Serum-Free Medium. *Vitr. Cell. Dev. Biol.* **26**, 589–595.

- Olsburgh, J., Harnden, P., Weeks, R., Smith, B., Joyce, A., Hall, G., Poulsom, R., Selby, P., and Southgate, J. (2003). Uroplakin gene expression in normal human tissues and locally advanced bladder cancer. *J. Pathol.* 199, 41–49.
- Osborn, S.L., Thangappan, R., Luria, A., Lee, J.H., Nolta, J., and Kurzrock, E. a (2014). Induction of human embryonic and induced pluripotent stem cells into urothelium. *Stem Cells Transl. Med.* 3, 610–619.
- Rudat, C., Grieskamp, T., Hr, C.R., Airik, R., Wrede, C., Hegermann, J., Herrmann, B.G., Schuster-Gossler, K., and Kispert, A. (2014). Upk3b is dispensable for development and integrity of urothelium and mesothelium. *PLoS One* 9.
- Shi, J.-G., Fu, W.-J., Wang, X.-X., Xu, Y.-D., Li, G., Hong, B.-F., Hu, K., Cui, F.-Z., Wang, Y., and Zhang, X. (2012). Transdifferentiation of human adipose-derived stem cells into urothelial cells: potential for urinary tract tissue engineering. *Cell Tissue Res.*
- Smith, N.J., Hinley, J.S., Varley, C.L., Eardley, I., Trejdosiewicz, L.K., and Southgate, J. (2015). The human urothelial tight junction: claudin 3 and the ZO-1 α + switch. *Bladder* 2, 9.
- Southgate, J., Hutton, K.A., Thomas, D.F., and Trejdosiewicz, L.K. (1994). Normal human urothelial cells in vitro: proliferation and induction of stratification. *Lab Invest* 71, 583–594.
- Strand, D.W., Degraff, D.J., Jiang, M., Sameni, M., Franco, O.E., Love, H.D., Hayward, W.J., Lin-Tsai, O., Wang, A.Y., Cates, J.M.M., et al. (2013). Deficiency in metabolic regulators PPAR γ and PTEN cooperates to drive keratinizing squamous metaplasia in novel models of human tissue regeneration. *Am. J. Pathol.* 182, 449–459.
- Subramaniam, R., Hinley, J., Stahlschmidt, J., and Southgate, J. (2011). Tissue engineering potential of urothelial cells from diseased bladders. *J. Urol.* 186, 2014–2020.
- Sun, T.T., Zhao, H., Provet, J., Aebi, U., and Wu, X.R. (1996). Formation of asymmetric unit membrane during urothelial differentiation. *Mol. Biol. Rep.* 23, 3–11.
- Tanaka, S.T., Ishii, K., Demarco, R.T., Pope IV, J.C., Brock, J.W., and Hayward, S.W.

(2010). Endodermal Origin of Bladder Trigone Inferred From Mesenchymal-Epithelial Interaction. *J. Urol.* *183*, 386–391.

The Cancer Genome Atlas Research Network (2014). Comprehensive molecular characterization of urothelial bladder carcinoma. *Nature* *507*, 315–322.

Tian, H., Bharadwaj, S., Liu, Y., Ma, P.X., Atala, A., and Zhang, Y. (2010). Differentiation of human bone marrow mesenchymal stem cells into bladder cells: potential for urological tissue engineering. *Tissue Eng. Part A* *16*, 1769–1779.

Turner, A., Subramanian, R., Thomas, D.F.M., Hinley, J., Abbas, S.K., Stahlschmidt, J., and Southgate, J. (2011). Transplantation of autologous differentiated urothelium in an experimental model of composite cystoplasty. *Eur. Urol.* *59*, 447–454.

Varley, C., Hill, G., Pellegrin, S., Shaw, N.J., Selby, P.J., Trejdosiewicz, L.K., and Southgate, J. (2005). Autocrine regulation of human urothelial cell proliferation and migration during regenerative responses in vitro. *Exp. Cell Res.* *306*, 216–229.

Varley, C.L., Stahlschmidt, J., Smith, B., Stower, M., and Southgate, J. (2004b). Activation of peroxisome proliferator-activated receptor-gamma reverses squamous metaplasia and induces transitional differentiation in normal human urothelial cells. *Am. J. Pathol.* *164*, 1789–1798.

Varley, C.L., Stahlschmidt, J., Lee, W.-C., Holder, J., Diggle, C., Selby, P.J., Trejdosiewicz, L.K., and Southgate, J. (2004a). Role of PPARgamma and EGFR signalling in the urothelial terminal differentiation programme. *J. Cell Sci.* *117*, 2029–2036.

Varley, C.L., Garthwaite, M.A.E., Cross, W., Hinley, J., Trejdosiewicz, L.K., and Southgate, J. (2006). PPARgamma-regulated tight junction development during human urothelial cytodifferentiation. *J. Cell. Physiol.* *208*, 407–417.

Varley, C.L., Bacon, E.J., Holder, J.C., and Southgate, J. (2009). FOXA1 and IRF-1 intermediary transcriptional regulators of PPARgamma-induced urothelial cytodifferentiation.

Cell Death Differ. 16, 103–114.

Wu, S., Cheng, Z., Liu, G., Zhao, X., Zhong, L., Zhu, Y., and Zhu, J. (2013). Urothelial differentiation of human umbilical cord-derived mesenchymal stromal cells in vitro. *Anal. Cell. Pathol.* 36, 63–69.

Yu, Z., Mannik, J., Soto, A., Lin, K.K., and Andersen, B. (2009). The epidermal differentiation-associated Grainyhead gene *Get1/Grhl3* also regulates urothelial differentiation. *EMBO J.* 28, 1890–1903.

Zhang, Y., McNeill, E., Tian, H., Soker, S., Andersson, K.E., Yoo, J.J., and Atala, A. (2008). Urine Derived Cells are a Potential Source for Urological Tissue Reconstruction. *J. Urol.* 180, 2226–2233.

Zhao, J., Zeiai, S., Ekblad, a, Nordenskjöld, a, Hilborn, J., Götherström, C., and Fossum, M. (2014). Transdifferentiation of autologous bone marrow cells on a collagen-poly(ϵ -caprolactone) scaffold for tissue engineering in complete lack of native urothelium. *J. R. Soc. Interface* 11, 20140233.

Table 1. List of primers used for RT-PCR and RT-qPCR.

Gene	Forward primer (5'-3')	Reverse Primer (5'-3')	Use
<i>ELF3</i>	GTTTCATCCGGGACATCCTC	GCTCAGCTTCTCGTAGGTC	RT-PCR
<i>ELF3</i>	TCAACGAGGGCCTCATGAA	TCGGAGCGCAGGAACTTG	RTqPCR
<i>FOXA1</i>	CAAGAGTTGCTTGACCGAAAGTT	TGTTCCCAGGGCCATCTGT	RT-PCR
			RTqPCR
<i>GATA3</i>	TCCAGACACATGTCCTCCCT	TGGTGTGGTCCAAAGGACAG	RT-PCR
<i>GATA3</i>	TCTATCACAAAATGAACGGACAGAA	TGTGGTTGTGGTGGTCTGACA	RTqPCR
<i>GRHL3</i>	GTGACAAGGGAGCTGAGAGG	CAGTCTCTGGCCGAAGGTAG	RT-PCR
<i>IRF1</i>	GCTGGGACATCAACAAGGAT	GTGGAAGCATCCGGTACT	RT-PCR
<i>KLF5</i>	GACACCTCAGCTTCCTCCAG	ACTCTGGTGGCTGAAAATGG	RT-PCR
<i>PPARG</i>	AGACAACCTGCTACAAGCCC	GGAAATGTTGGCAGTGGCTC	RT-PCR
<i>PPARG</i>	GAACAGATCCAGTGGTTGCAG	CAGGCTCCACTTTGATTGCAC	RTqPCR
<i>UPK1A</i>	GGGGTATCTCGTGGTTTGGG	CGTAAGGGCTAGGGACGTTG	RT-PCR
<i>UPK1A</i>	CATTCTTGCTGAACCGTTTGTG	GTGACCGTGACAGAACTCTCATG	RTqPCR
<i>UPK1B</i>	TTGAAGCCACCGACAACGAT	AACAGACAGGCAGAAGAGGC	RT-PCR
<i>UPK1B</i>	CGCTTGCCTTCAGCTTGTG	GGCCCTGGAAGCAACGA	RTqPCR
<i>UPK2</i>	CTCCCGCAAGTAAGGAGGT	GAAGGATGGGGGAATTGTTA	RT-PCR
<i>UPK2</i>	CAGTGCCTCACCTTCCAACA	TGGTAAAATGGGAGGAAAGTCAA	RTqPCR
<i>UPK3A</i>	ATGGGGAGTTCTGATGGGGA	TGCTGGAATACACCTCAGCC	RT-PCR
<i>UPK3A</i>	CGGAGGCATGATCGTCATC	CAGCAAACCCACAAGTAGAAAGA	RTqPCR
<i>UPK3B</i>	CCTCCTGCTTCACTCTCTGTCT	GAAACTGACAATCACGGCAGAA	RT-PCR
			RTqPCR
<i>GAPDH</i>	CAAGGTCATCCATGACAACCTTG	GGCCATCCACAGTCTTCTG	RT-PCR
			RTqPCR

Figure Captions:**Figure 1. Comparison between buccal epithelium and urothelium *in situ* and *in vitro*.**

(A-B) Histological sections showing representative *in situ* immunolocalisation patterns for cytokeratins CK5, CK7, CK13, CK14 and CK20 in (A) buccal mucosa (scale bar \equiv 100 μ m) and (B) urothelium (scale bar \equiv 25 μ m).

(C) Representative phase contrast images of NHB and NHU cells grown *in vitro*. (Scale bar \equiv 200 μ m)

(D) Immunofluorescence microscopy images of cytokeratin CK5, CK7, CK13, CK14, and CK20 expression by NHB and NHU cells grown in low calcium, serum-free medium (KSFMc). Immunolabelling was performed on n=3 independent NHB cell lines and images are representative, although note that CK13+ cells are infrequent in NHU cell cultures grown in these non-differentiated conditions. Scale bar \equiv 50 μ m.

Figure 2. Formation of cell sheets and barrier function. The ability to form a stratified barrier epithelium was examined in three independent NHB cell lines, with a representative NHU cell line provided for comparison purposes.

(A) Representative hematoxylin and eosin-stained NHB and NHU cell sheets showing multi-layered tissue structures formed 7 days post-seeding onto membranes in serum- and 2 mM calcium-containing medium. Scale bar \equiv 100 μ m.

(B) Trans-epithelial electrical resistance (TEER) measurements taken daily. Day 0 measurements were taken 24 hours after seeding the cells onto membrane inserts, directly before the medium was changed to increase the calcium concentration to 2 mM.

(C) Immunohistochemical analysis of NHB and NHU cell sheets for CK5, CK7, CK13 and CK14 protein expression. Representative results shown from experiments performed on n=3 independent NHB cell lines. Scale bar \equiv 50 μ m.

Figure 3. Comparison of uroplakin and urothelium differentiation-associated transcription factor gene expression by NHB and NHU cell cultures. Employing protocols developed to differentiate NHU cells by PPAR γ activation, cell cultures of NHB or NHU cells were exposed to 1 μ M troglitazone and 1 μ M PD153035 (TZ/PD) for 24 hours, maintained in 1 μ M PD153035 and harvested at 12, 24, 48 and/or 72 hours. Control cultures were exposed to vehicle (0.1 % DMSO) alone.

(A) RTqPCR for three independent NHB cell lines (represented by different symbols), versus a single NHU cell line for comparison of uroplakin (*UPK1A*, *UPK1B*, *UPK2*, *UPK3A* and *UPK3B*) mRNA expression at the 72 hour time-point. All data has been normalised to GAPDH expression and is presented relative to the DMSO-treated NHB cells for each gene except *UPK3A*, where the data is shown relative to the DMSO treated NHU cells due to absent *UPK3A* gene expression by NHB cells. BLOD = Below Limit of Detection. Statistical analysis was performed using a two-tailed, paired t-test to determine whether TZ/PD resulted in any significant change in gene expression in NHB cells.

*represents $P \leq 0.05$, ** represents $P \leq 0.01$. Error bars represent standard deviation

(B-C) RT-PCR of *ELF3*, *FOXA1*, *GATA3*, *GRHL3*, *IRF1*, *KLF5* and *PPARG* mRNA expression by (B) NHB cells and (C) NHU cells. RNA was extracted at the 12, 24 and 48 hour time-points and then DNAase-treated and used to generate cDNA for RT-PCR. *GAPDH* used as an internal loading control. A no-template (H_2O) control was included as negative control for the PCR reaction and genomic DNA was used as the positive control (+ctrl). No product amplified from RT-negative controls (not shown). Experiments were performed on n=2 independent NHB donor cell lines and representative results shown.

Figure 4. Evaluation of ELF3, FOXA1, GATA3 and PPARG expression in NHB cells.

RNA and protein were extracted from parallel cultures of NHB and NHU cells at 72 hours following exposure to the PPAR γ -activating TZ/PD protocol, or a vehicle control (0.1% DMSO).

(A) RTqPCR results combined from three independent NHB cell lines (represented by different symbols), with a single NHU cell line for comparison. All data is normalised to *GAPDH* expression and is presented relative to the DMSO-treated NHB cell control for each gene. Statistical analysis was performed using a two-tailed, paired t-test to test if TZ/PD treatment resulted in any significant change in gene expression in NHB cells. ** represents $P \leq 0.01$. Error bars represent standard deviation.

(B) Immunoblot of whole cell protein lysates from representative NHB and NHU cell cultures following exposure to the TZ/PD protocol, 1 μ M PD153035 alone, or vehicle (0.1 % DMSO) for 72 hours. ACTB is included as an internal loading control. Experiments performed on n=3 independent NHB cell lines with similar results.

(C) Immunofluorescence microscopy of ELF3, FOXA1/2, GATA3 and PPAR γ in representative NHB and NHU cell cultures. Images taken at identical exposures to demonstrate differences in labelling intensity between the two cell types. Experiments performed on n=3 independent NHB donor cell lines with similar results. Scale bar \equiv 50 μ m.

Figure 5. GATA3 overexpression in NHB cells.

(A) *GATA3* overexpressing and control (empty vector) NHB cell cultures following exposure to the PPAR γ -activating TZ/PD protocol for 72 hours. Western blotting of whole protein lysates was performed to assess protein expression of GATA3, FOXA1 and PPARG1. NHU

cells (non-transduced) and treated with the TZ/PD protocol for 72 hours are shown for comparison.

(B) *GATA3* overexpressing and control (empty vector) NHB cells at 72 hours post TZ/PD protocol. *GATA3*, *FOXA1* and *PPARG* protein expression assessed by indirect immunofluorescence microscopy. NHU cells (non-transduced; 72 hour TZ/PD protocol) were included as positive controls for comparison. Scale bar = 50 μ m.

(C) *GATA3* overexpressing and control (empty vector) NHB cells were induced to form cell sheets using 5 % ABS and 2 mM calcium for up to 7 days. Expression of the tight junction-associated proteins, Claudin 3, 4, 5 and 7, assessed by western blotting. *ACTB* was included as a loading control. NHU cells (non-transduced) exposed to the same protocol were used as a positive control for comparison.

Experiments were performed on n=2 independent NHB donor cell lines and representative results shown.

Figure 6. Evaluation of *PPARG*, *FOXA1* and *GATA3* expression in *PPARG1*

overexpressing and control (empty) NHB cells. *PPARG1* overexpressing and control (empty vector) NHB cell cultures were exposed to the TZ/PD protocol for 72 hours.

Experiments performed on between 2 to 4 independent NHB cell lines (as stated below), with representative results shown.

(A) *PPARG1*, *FOXA1* and *GATA3* protein expression assessed by western blotting. *ACTB* expression included as internal loading control. Protein lysates from cell lines known to express the proteins of interest were included as positive controls for each antibody (CTRL). Experiments performed on n=3 independent NHB cell lines.

(B) Densitometry analysis of *FOXA1* protein expression shown relative to control (Empty - DMSO) NHB cells. Data is shown as the mean of n=4 independent transduced NHB cell

lines. All values normalised to the ACTB expression. Statistical analysis was performed using a one-way ANOVA test, but no statistical significance was found ($P > 0.05$). Error bars represent standard deviation.

(C) Immunofluorescence microscopy evaluating PPAR γ , FOXA1 and GATA3 protein localisation in PPAR γ 1 overexpressing and control (empty vector) NHB cells following the TZ/PD protocol at 72 hours. Experiments were performed on $n=3$ independent transduced NHB cell lines. IF images for a single NHB cell line are shown. Nuclear localisation was observed with PPAR γ ($n=3/3$), FOXA1 ($n=3/3$), and GATA3 ($n=2/3$). NHU cells (non-transduced) treated with the TZ/PD protocol are shown for comparison at the same time point. Scale bar = 50 μm .

Figure 7. Assessment of tight junction-associated proteins and CK14 expression in PPAR γ 1 overexpressing and control (empty) NHB cells. PPAR γ 1 overexpressing and control (empty vector) transduced NHB cells were induced to stratify using serum and calcium (detailed in the Methods). Experiments were performed on $n=3$ independent NHB donor cell lines. Results at 7 days shown for a representative transduced NHB cell line. ACTB expression used as internal loading control. NHU cells (non-transduced) exposed to the same protocol for 5 days are shown for comparison.

(A) Evaluation of tight junction-associated protein expression by western blotting with Claudins 3, 4, 5 and 7.

(B) Densitometry analysis of claudin 3 expression at day 7 shown relative to control (empty vector) cells. All values were normalised to the ACTB expression. Data is shown as the mean of $n=3$ independent transduced NHB donor cell lines. Statistical analysis performed using a two-tailed, paired t-test. * represents $P \leq 0.05$. Error bars represent standard deviation.

(C) CK14 expression evaluated by western blotting.

Supplementary Figure 1. Assessment of uroplakin gene expression by NHB and NHU cells *in vitro*.

(A-B) RT-PCR of uroplakin (*UPK1A*, *UPK1B*, *UPK2*, *UPK3A* and *UPK3B*) mRNA expression by (A) NHB and (B) NHU cell lines on RNA extracted at 12, 72 and 144 hours following treatment with TZ/PD. *GAPDH* was included as a housekeeping gene. RNA was digested with DNAase to remove any genomic DNA contamination and tested as RT-negative controls (not shown). Other shown controls include a no-template (H₂O) negative and a genomic DNA positive control (+ctrl). Experiments were performed on n=2 independent NHB cell lines with similar results.

Accepted manuscript

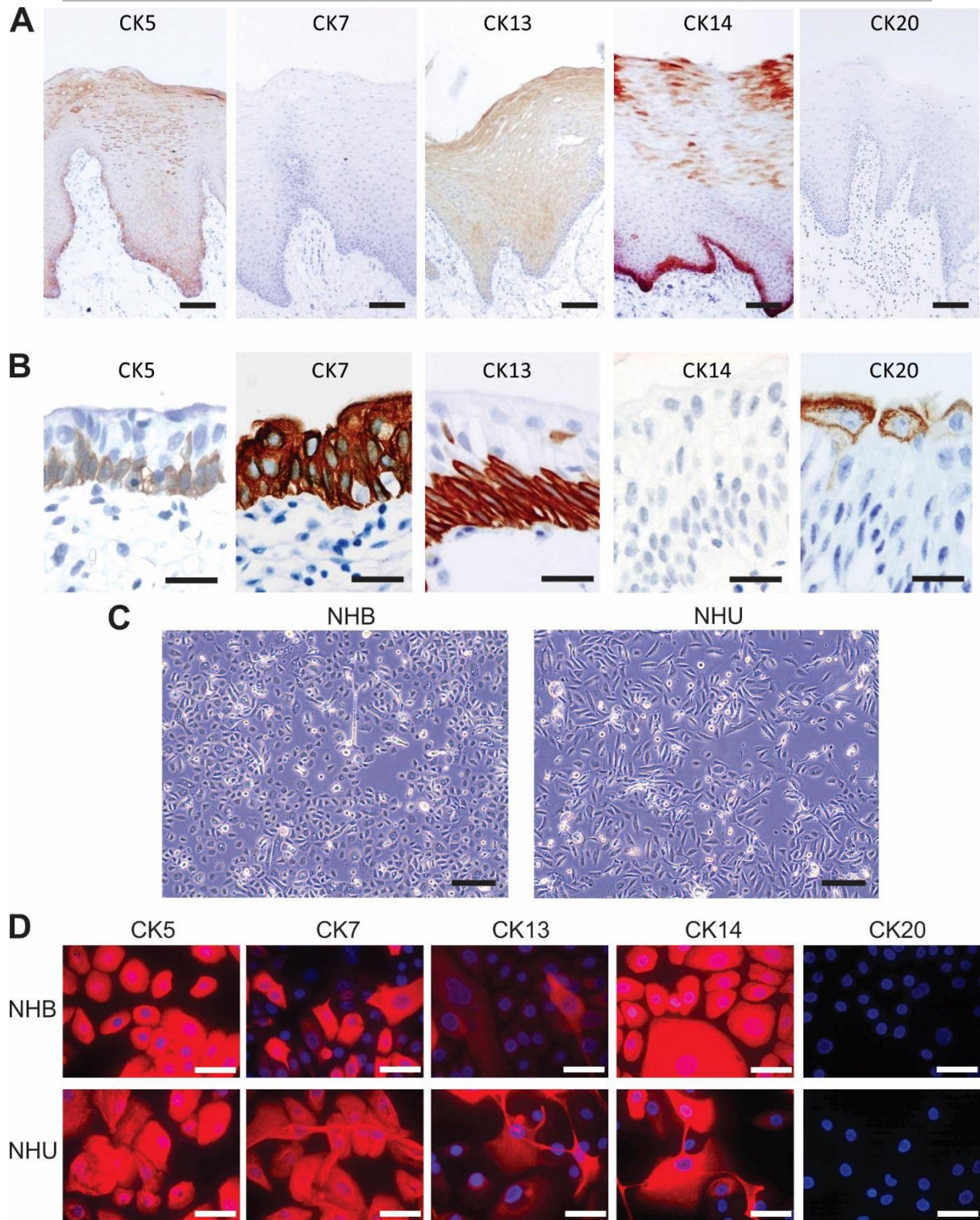


Figure 1

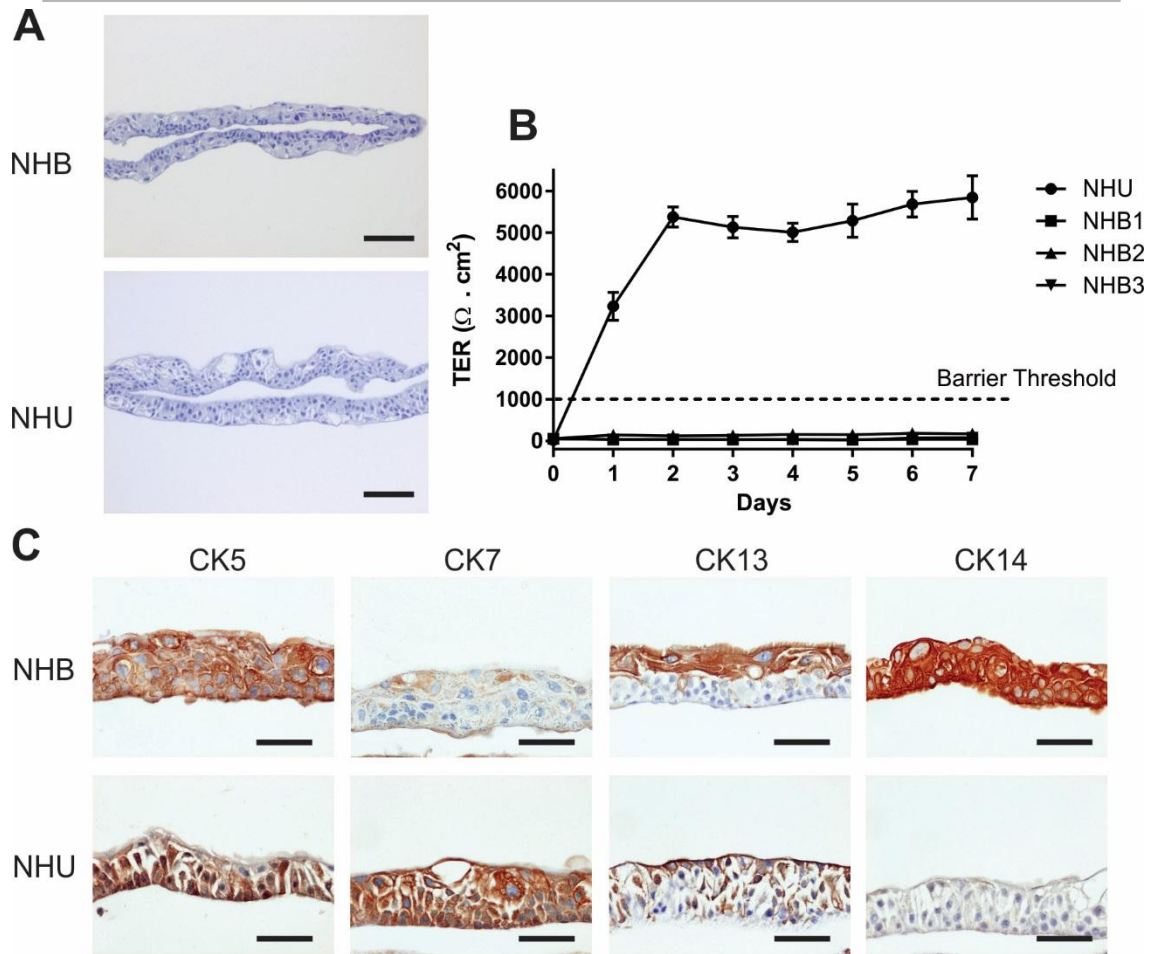


Figure 2

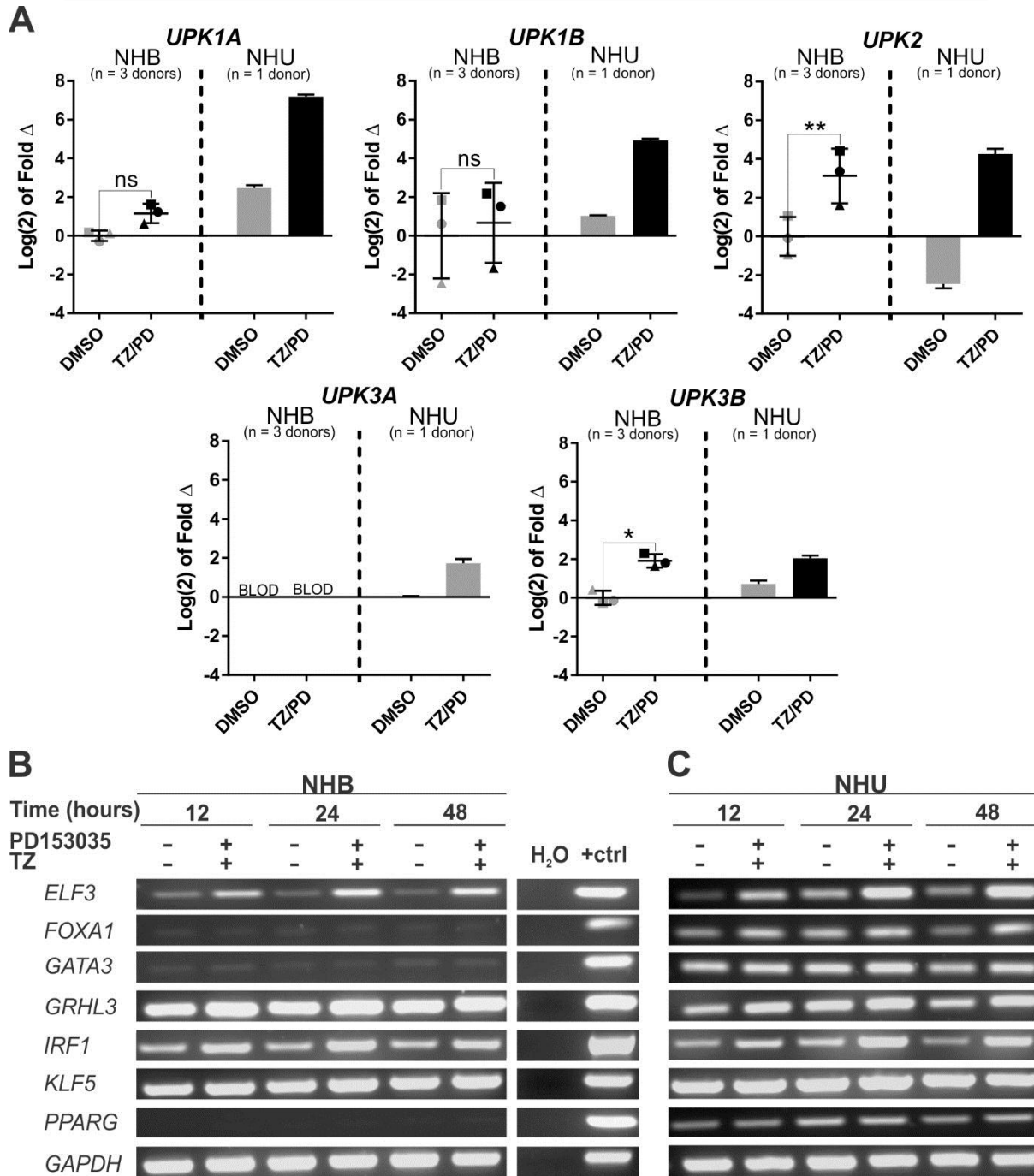


Figure 3

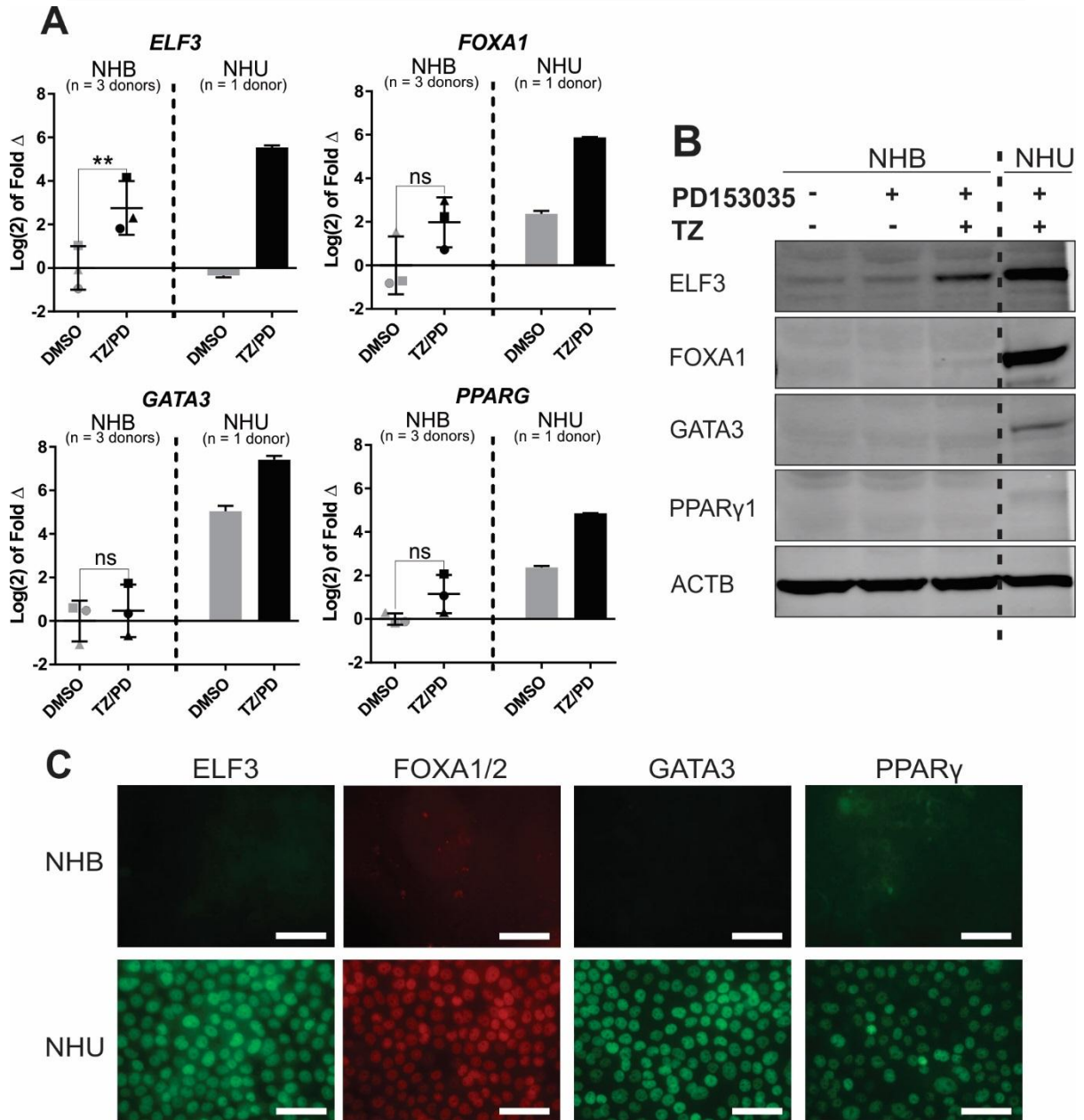


Figure 4

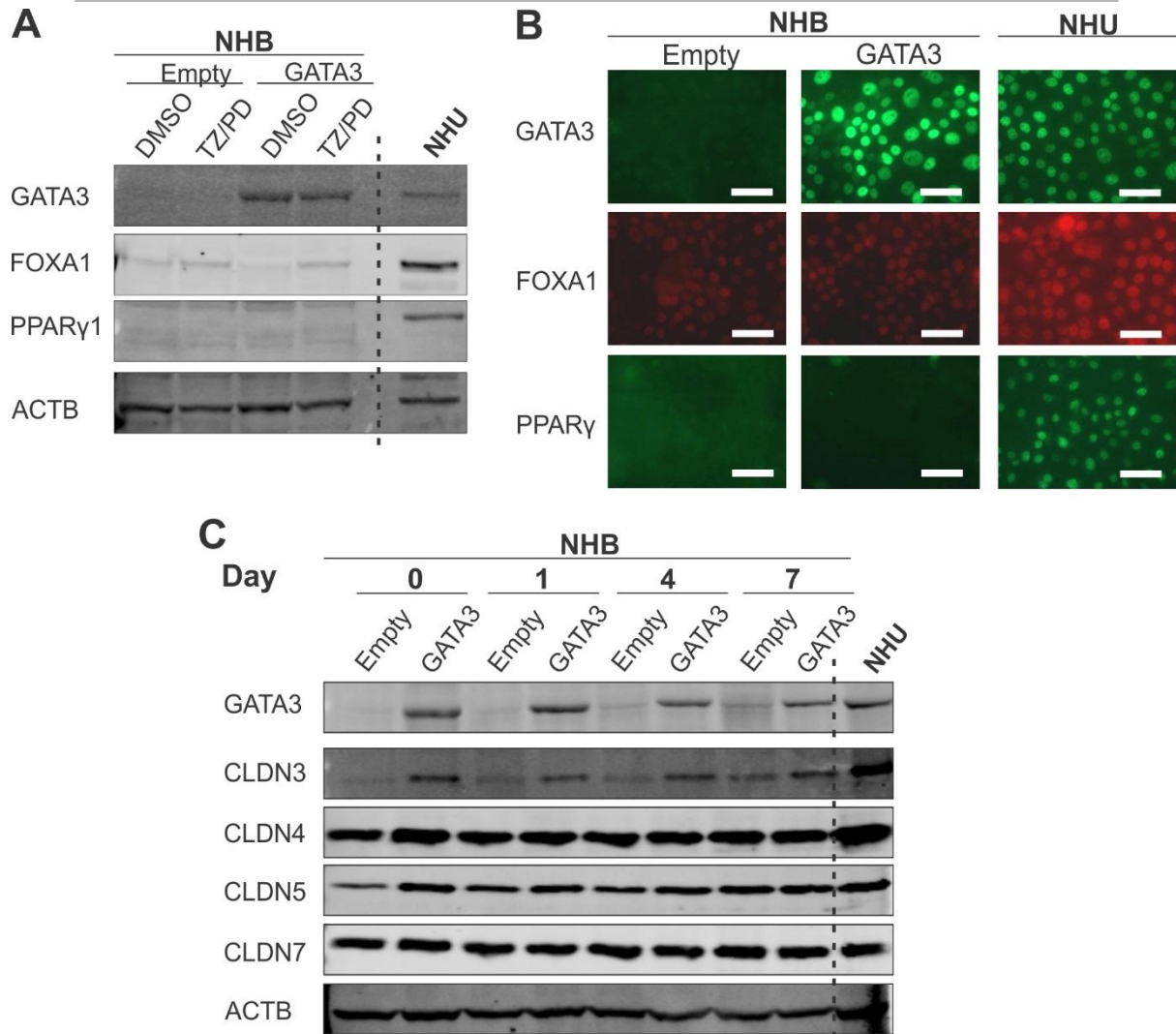


Figure 5

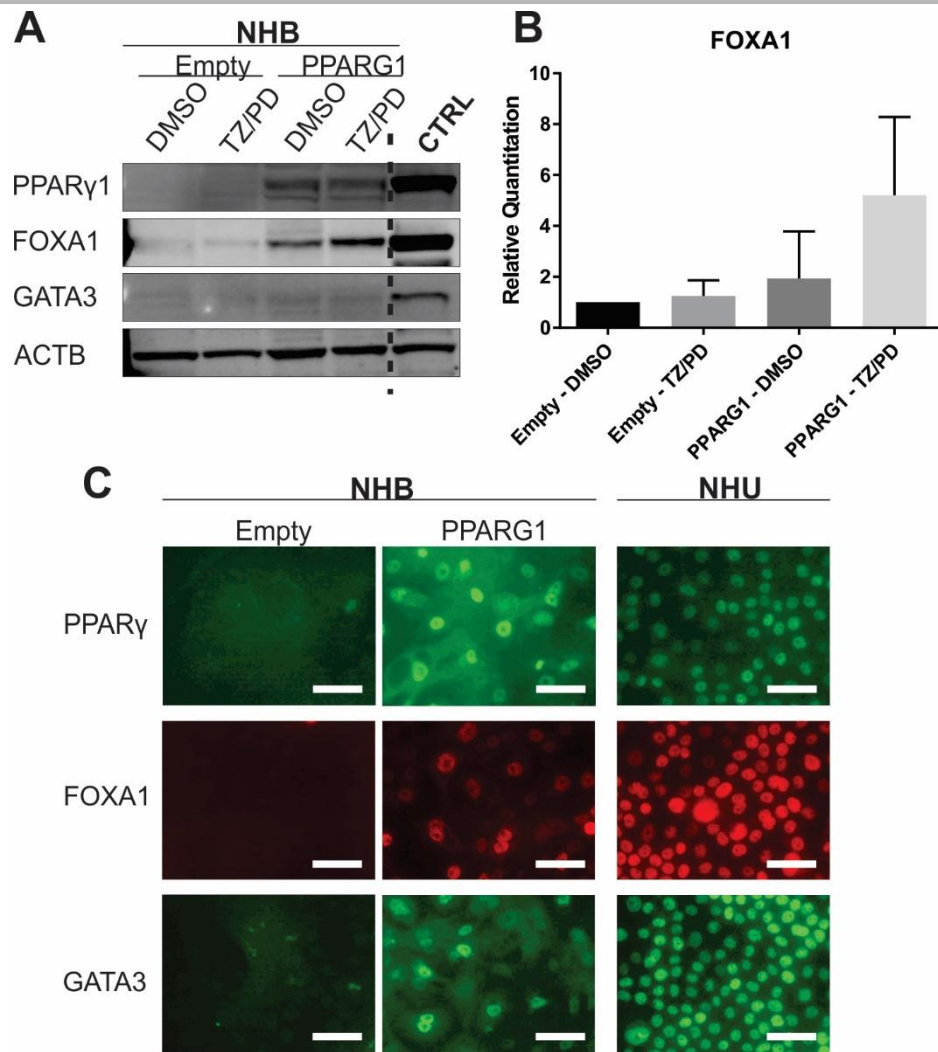


Figure 6

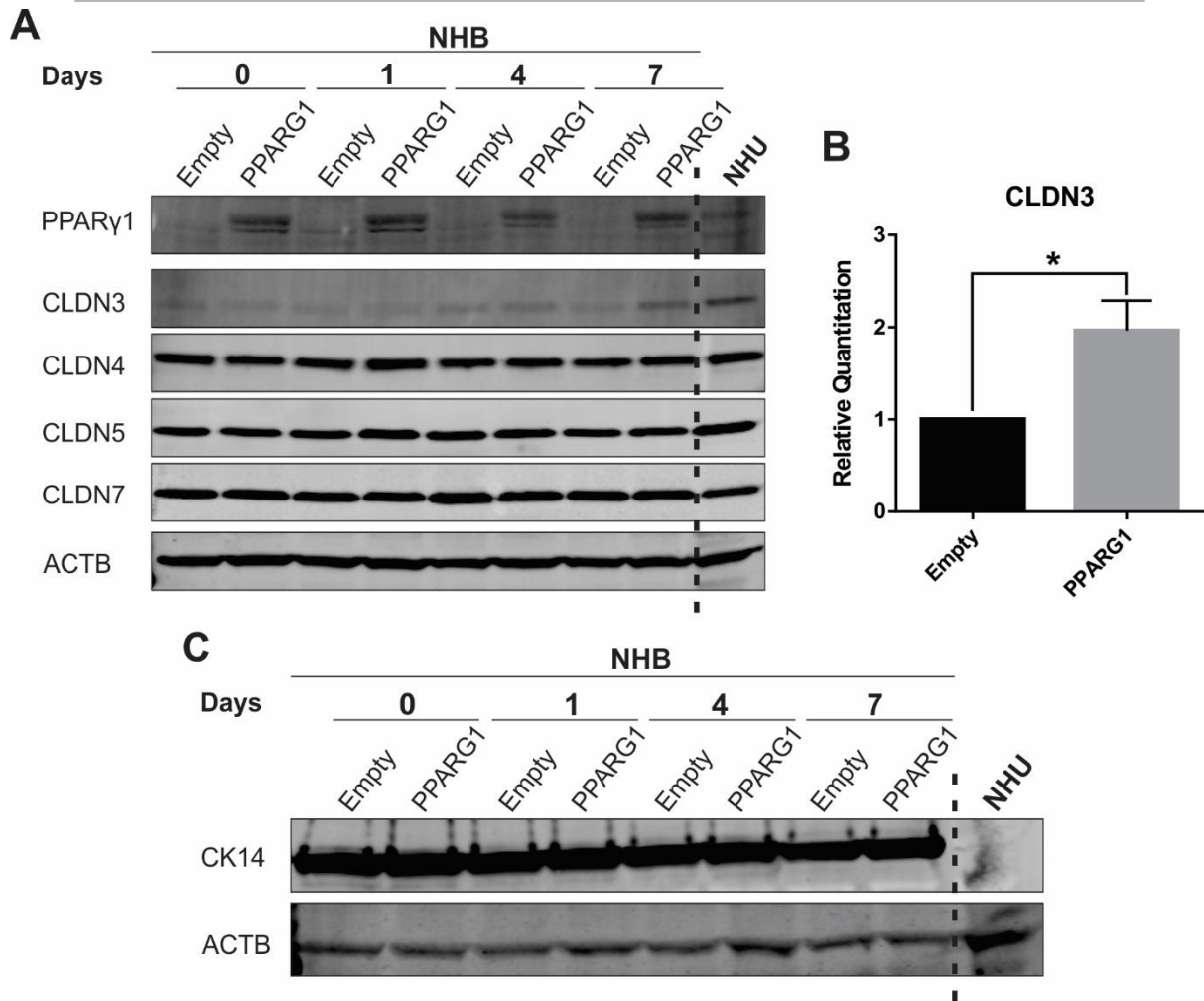
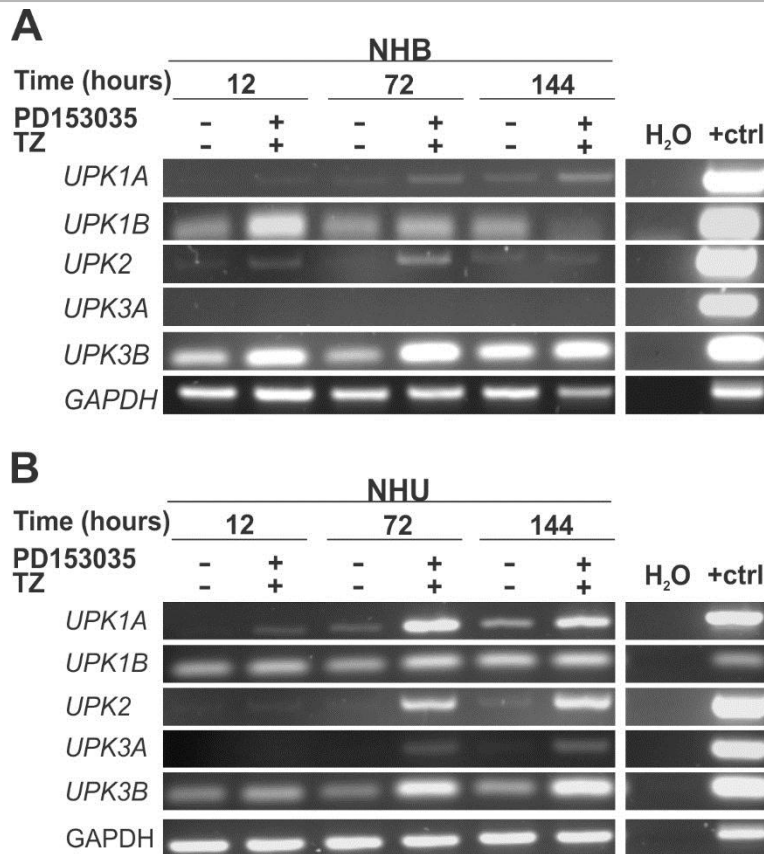


Figure 7



Supplementary Figure 1